INSTITUTE OF PLASMA PHYSICS

NAGOYA UNIVERSITY

Efficient Heating and Confinement of Ions in An Axisymmetric Magnetic Mirror Supplemented with DC Electric Field

Y. Nishida, H. Mase and K. Ishii

(Received – Oct. 17, 1984)

IPPJ- 707 Dec. 1984

RESEARCH REPORT

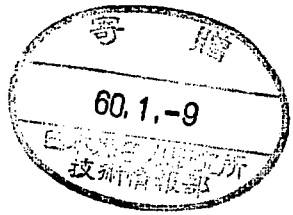

NAGOYA, JAPAN

Efficient Heating and Confinement of Ions in an Axisymmetric Magnetic Mirror Supplemented with DC Electric Field

Y.Nishida*, H.Mase** and K. Ishii

(Received - Oct. 17, 1984)

IPPJ - 707 Dec. 1984

Further communication about this report is to be sent to the Research Information Center, Institute of Plasma Physics, Nagoya University, Nagoya 464, Japan.

Permanent address:

* Department of Electrical Engineering, Utsunomiya University, Utsunomiya, Tochigi 231, Japan.

** Department of Electronic Engineering, Ibaragi University, Hitachi, Ibaragi, 316, Japan.

EFFICIENT HEATING AND CONFINEMENT OF IONS IN AN AXISYMMETRIC MAGNETIC MIRROR SUPPLEMENTED WITH DC ELECTRIC FIELD

Y.Nishida*, H.Mase**, and K.Ishii
Institute of Plasma Physics, Nagoya University
Nagoya. Aichi 464. Japan

Strong heating and improved confinement of ions have been observed in an axisymmetric magnetic mirror field supplemented with an electrostatic DC field across and along the magnetic field lines. The increased life time of ions is understood as trapping of ions in the electrostatic potential well in the magnetic mirror field. The efficient heating of ions is resulted from the thermalization through weak collisions and/or finite correlation time of the strong EXB type instabilities excited by the radial current flowing into the outer electrode. The ion temperature increases in proportion to V_H^2, the square of the applied DC voltages for heating.

I Introduction

It is strongly expected to clarify plasma-wall interaction phenomena for improved confinement and heating of particles in a magnetically confined plasma (Alikhanov et al, 1970; Alikhanov and Konkashbaev, 1974). In addition, it is also expected to develop a new system which is useful for efficient heating and confinement of plasmas, as well as an elaborated "Tokamak system" (Fowler, 1981) which, however, is one of the most plausible candidate for fusion reactor devices. There is an open sytem as another trend, such as "Tandem Mirror system" (Fowler, 1981; Dimov et al, 1976), which is also expected to be a future fusion reactor device.

In the previous paper (Nishida et al, 1975; 1977), we have presented the experimental results on the increased confinement of ions in a simple magnetic mirror system supplemented with DC electric field. We also have observed an efficient heating of ions in the same system (Nishida et al, 1979). In the present paper, we would like to show further experimental results of the investigations for an efficient heating and improved confinement of ions for clarifying the physical mechanisms in an axisymmetric simple mirror device supplemented with DC electric field which is applied externally across and along the magnetic field lines. This system consisting of a combination of magnetic mirror and static potential well has been developed for investigating the heating and confinement mechanisms of ions in a small system.

In the past years, cross-field-current driven microinstabilities have been intensively studied, particularly in connection with anomalously high efficient heating of ions in a plasma with

a relativistic electron beam injected into the mirror machine (Alexeff et al, 1970) and in the modified Penning discharge (Roth, 1973). Among these instabilities, a lower hybrid instability, with a frequency between an electron and ion cyclotron frequencies, is easily destabilized by an EXB current. This instability has been proved to be able to play an important role in an enhanced ion heating. On the other hand, some of the experiments have shown that the heating mechanism in the similar type of the machine mentioned above is regarded as the joule heating due to the collisional thermalization of the kinetic energy of the EXB drift motion generated by the radial current (Nishida et al, 1977; 1979; Sugai, 1977). Thus, we have to clarify the differences of the basic process in the heating mechanism of ions. In addition, we have confirmed the increased ion confinement by performing direct measurements of the particle confinement time.

In section II, the experimental set-up is described and experimental results are given in Sec.III. The results are discussed in Sec.IV and summarized in Sec.V.

II Experimental set-up

The present experiments were performed on the "TPD-I" machine (Takayama et al, 1967) at Institute of Plasma Physics, Nagoya University. A schematic description of the experimental set-up is shown in Fig.1, which is essentially the same as that shown in the references (Nishida et al, 1975; 1977) except for the size of the chamber of the heating section. The axisymmetric

magnetic mirror field in the experimental section (denoted as I) has the maximum strength of 2.5 kG at the center of the mirror field with a fixed mirror ratio R $\simeq$ 1.9. The helium plasma produced in the source section (denoted as II) with uniform magnetic field structure has the maximum density n_e of about 3×10^{14} cm^{-3} at the column center with an electron temperature T_e $\simeq$ 10 eV in a neutral gas pressure of P $\simeq$ 2×10^{-3} Torr. This plasma diffuses into the experimental section through an orifice O_o, where the plasma density decreases to the maximum value of n_e $\simeq$ 1×10^{13} cm^{-3} in 7×10^{-5} Torr $\leqq$ P $\leqq$ 1×10^{-3} Torr, and both of electron and ion temperatures are 30-50 eV. For measuring the transient state, the electric current for sustaining a plasma production is chopped electrically with repetition rate of 10 Hz and about 50% duties. The characteristic decay constant of the electric current is less than about 20 μsec.

There are four kinds of orifices installed within a vacuum chamber, denoted O_o, O_2, O_3 and O_4, but O_3 and O_4 are essentially identical. O_2 is made of metallic plate with a hole diameter of 3 cm and O_3 is of ceramic plate with a hole diameter of 2 cm. The orifice O_2 is biased to positive by an external power supply, denoted as V_o, against the plasma potential, or it is left to the floating potential. The orifice O_3 works to protect the electrode O_2 from direct bombardment of the plasma flowing in from the source region and so to reduce the electric coupling. The hole diameter of O_2 should always be larger than that of O_3, because of reducing the direct electrical coupling of the annular electrode with the plasma source along the magnetic field lines. This is essential for efficient heating and confinement of ions

in the trapping section.

The cylindrical chamber made of stainless steel can be biased up to 3 kV by the external DC power supply, denoted as V_H, against the ground potential which is close to the plasma potential. The magnetic field line which touches the edge of the hole of O_3 is designed not to go into the annular electrode directly, so that the direct coupling of the particles flowing along the magnetic field lines is reduced to the minimum amount. This is essentially the same effect as that mentioned above.

An ion temperature, T_i, is determined from a full-half width of the Doppler broadening of HeII (4686 Å) line, by using a double-monochrometer. The ion temperature thus obtained is a perpendicular component to the magnetic field lines. A parallel component of T_i cannot be observed in the present machine because of the machine restriction, although we have tried to measure it by using several mirrors for failure to obtain meaningful results. Plasma instabilities are observed by using a Langmuir probe and a floating double-probe, both being movable across and along the plasma column within the trapping section.

III Experimental Results

It has been confirmed that the ion confinement in a magnetic mirror field is improved, when a positive voltage, V_H, for heating ions is increased up to certain voltages (Nishida et al. 1977). For further increasing of the heating voltage, however, the plasma breakdown occurs to abrupt increase of the ion current flux, I_{out}, through the orifice, O_2, and also the electric cur-

rent, I_H, for heating the plasma, where I_{out} is used as a measure of the ion confinement as will be shown later. Here it is important how we can suppress the plasma breakdown and so how we can apply high enough voltages to the cylindrical electrode, otherwise we cannot obtain the good heating efficiency and high ion temperature. For these purposes, we have tried the discharge cleaning method for cleaning the cylindrical electrode and both orifices of O_2 for severals of 10 times before taking data. As a result, a lot of impurities from the cylindrical electrode were ejected and finally the plasma breakdown became rather hard to occur, still the maximum voltage applicable to the plasma is restricted by the breakdown. An example of the decreased loss of ion flux through the orifice, O_2, is shown in Fig.2, where the loss factor $\delta = I_{out}(V_H)/I_{out}(0)$ is a function of the applied voltage, V_H, for heating ions and I_{out} is an ion saturation current of the probe P_2. δ can be decreased to roughly 1/5-1/8 which is independent of the probe bias voltages. The final state is limited by the plasma breakdown as is mentioned above. The breakdown voltage decreased with an increase of the plasma density as is also seen in Fig.2. Once the breakdown starts, a lot of impurities, mainly, of FeII are observed within the plasma, i.e. the impurities mainly may come from the cylindrical electrode, although we cannot determine the spatial profile of the impurity ions in the present diagnostic method.

When the breakdown in the plasma does not occur, an ion temperature is determined from the Doppler broadening of HeII (4686 Å) line as an example is shown in Fig.3. This figure shows raw data of the line spectra around HeII line observed through

the plasma column at the center of the magnetic mirror field. In this example strong instabilities make noisy figure in the spectrum line, but we can obtain Fig.4 after averaging the data such as shown in Fig.3. In Fig.4, $\Delta\lambda$ is a difference of the wave length measured from HeII line. It is clearly seen that there are two components in the ion temperature, bulk cold component and hot component. Both of the ion components, however, show good linear relationship in each region as seen in Fig.4, showing reasonably good Boltzmann distribution in each component. From this kind of figure shown in Fig.4, we can obtain an ion temperature as a function of the heating voltage V_H applied across the plasma column on the cylindrical electrode as shown in Fig.5. This shows that the hot component of ion temperature increases with V_H^2, but the temperature in a cold bulk component does not change very drustically.

It has been clarified that a cold component comes from the plasma source and exists mainly in a plasma column axis region, while a hot ion component existing off axis in the trapping region has been clarified to be heated up by the radial current J_r induced by the crossed electric field. We can obtain an empirical relationship between the ion temperature of the hot component and the heating voltage V_H as;

$$T_i = KV_H^2 + T_{io}, \qquad (1)$$

where K is a positive constant and T_{io} is an initial ion temperature determined by the plasma source without heating voltages. The electron temperature T_e is also measured by using a Langmuir probe in a low plasma density condition. T_e is almost constant

to be about 30-50 eV for $V_H \leqq 1.2$ kV. In another words, strong heating of electrons did not occur.

The plasma breakdown voltage, V_B, has been clarified to depend on the neutral gas pressure, P, as an example is shown in Fig.6. Here we used several cylindrical electrodes with different radius, r. Unfortunately, we cannot obtain the magnetic field dependence of the data. From this result we can obtain the empirical relation of

$$V_B/P^n r = \text{constant} \qquad (2)$$

with $n \simeq 0.45$-0.47. Most of the applied DC voltages exist in front of the annular electrode to form a sheath region of thickness of about 2-3 cm depending on the plasma conditions. The breakdown seems to start in this sheath region, although it is not identified exactly.

A particle confinement time has been observed by chopping the source plasma for measuring a decay time of the plasma with a floating double probe in the trapping section. A typical example of the decay time τ is shown in Fig.7, in which the decay time is seen to depend on the radial position if it is measured either outside or inside of the center column region of about 2.5 cm in diameter. In the region close to the column center ($r \simeq 1$ cm), τ increases slightly with a heating voltage V_H, while it increases more than 8-10 times than the initial state of $V_H = 0$ at $r \simeq 7$ cm. More precisely, the decay time of initially 100-200 μsec increases to about 1.5-2.0 msec at V_H = 100-200 volts without significant increases of ion temperature in both cases of r = 1 cm and 7 cm. Further increase of the heating voltage decreases the decay time once and then increases it again, espe-

cially in the outer region such as r = 7 cm as seen in Fig.7(b). This may be reasonable because the particles existing in the outer off-center region are trapped electrostatically as the potential well develops with the heating voltages in the magnetic mirror field as is anticipated (Nishida et al, 1975; 1977). In a transient state of the after-glow plasma, the radial current J_r drawn by the crossed field E_r for heating ions has been shut off much quickly compared with the plasma decay time of the order of 1 msec, and so the ionization of the residual neutral gas caused by hot electrons existing in an ionization phase for sustaining the plasma density is negligibly small not to be effective for changing the decay time τ within the trapping section. Short decay time observed in the range of 200 V $\leqq V_H \leqq$ 1300 V has relations with instability strength, which will be discussed later. For $V_H \leqq$ 200 V, an amplitude of the observed instability is quite small and the decay time τ increases up to about 1-2 msec, but once the instabilities set in very strongly, the decay time decreases to about 0.4 msec. For further increase of V_H, the confinement efficiency increases to overcome the plasma loss caused by the instabilities and the decay time increases again to about 1 msec. This feature is clearly seen in Fig.7(b), while in Fig.7(a), which is observed near the plasma core, the plasma is blown off toward the trapping section and the increase of confinement time is not observed anymore even in large V_H regions.

In the trapping section strong instabilities have been observed as an example of the frequency spectrum is shown in Fig.8,

in which an instability with frequency of typically 200 kHz is observed. The wave strength increases with V_H and its spectrum becomes turbulent like in larger voltage regions. The instability with largest amplitude is investigated precisely as well as the special frequency range of a lower hybrid resonance frequency, ω_{LH}. In the present experiment, however, any instability with lower hybrid frequency range has not been observed, at least, an instability with distinct amplitude is not observed at all in this frequency range. The frequencies of the observed instabilities change with the applied magnetic field strength and the DC voltage. Here, the radial electric field strength, E_r, has been clarified to be almost proportional to V_H (Nishida et al, 1977). The parametric dependence of the present instabilities are shown in Fig.9, where m-number shows the azimuthal mode number, I_d is the discharge current in the source plasma region and is roughly proportional to the plasma density. In the z-direction any discrete wave number has not been observed and $k \sim 0$ could be assumed. Here, the magnetic field density is measured at the center of the magnetic mirror field. As clearly seen from Fig.9, m = 2 mode is observed in the wide variety of parameter regions compared with m =1 mode, and both modes are essentially E X B type instabilities. In Fig.9, only two modes are presented, but in some parameter regions, the higher modes up to m = 6 have been observed.

IV Discussion

If there is a weak collision of ions, including ion-neutral and ion-ion collisions, in a crossed electric and magnetic field

system, the dispersion relation for this kind of instability can be obtained (Saito et al, 1966; Nishida et al. 1968; Nishida and Hatta, 1970) in a cartesian coordinate system,

$$\omega \simeq k_\perp \cdot V_{eo} + ik_\perp \cdot V_{eo} \left(\frac{k_x \cdot L}{k_\perp^2} + \frac{\nu_i}{\omega_{ci}} \frac{k_\perp^2}{k_y L} \right) - i \frac{m}{M} \nu_i \rho_i^2 k_\perp^2, \quad (3)$$

where $K_\perp \cdot V_{eo} = k_x V_{xo} + K_y V_{yo}$, $V_{yo} = cE_{xo}/B_o$ is the steady state cross-field drift velocity, V_{xo} is the drift velocity in the radial direction originated from the density gradient in the radial direction and from the drift current for heating plasma; the latter effect is dominant in an appropriately stronger DC field, V_H. $L = \partial \ln n_o / \partial x$ is the density gradient scale length in the radial direction and $k_\perp^2 = k_x^2 + k_y^2$, ν_i is the collision frequency, ω_{ci} is an ion cyclotron frequency and ρ_i is an ion Lamor radius. Here, the instability has small wave number k_x in the direction of the density gradient. In a present parameter region, $k_y V_{yo} > k_x V_{xo}$ is held as is also expected in the present model. As seen from Eq.(3), the small ion collision and the density gradient in the x-direction ($L > 0$) cause to excite the present instabilities with the aid of azimuthal drift velocity, while the finite ion Larmor radius effect shown by the last term in Eq.(3) works to stabilize the present mode. The electric field obtained near the plasma column center is used for calculating the frequency and the result is shown by solid lines in Fig.9, showing reasonably good agreement with the experimental results. Here, k_y is calculated as $k_y = m/r_o$, and r_o is the radial position of the maximum amplitude, and the electric field strength is also measured around here. In the high heating

voltage range more than about 500 V, we cannot measure directly the radial electric field strength and assumed that the electric field is proportional to V_H as it is in the lower voltage range. Thus, the strong plasma rotation in the azimuthal direction may excite the E X B type instability mainly with azimuthal mode number of m = 2 which has the maximum growth rate in the present conditions.

The electric power fed from the DC power supply applied on the heating electrode is dissipated through the radial current $J_r = enV_{eo} = en(\nu_i/\omega_{ci} + \nu_e/\omega_{ce})cE_{xo}/B_o$ into the ion thermal motion by a small number of collisions or strong fluctuating electric fields induced by the strong instabilities. In the present machine an ion confinement time is about 1 msec, which is even larger than the ion collision time (ion-neutral, or charge exchange collisions). Furthermore there is a possibility that the fluctuating electric fields originated in E x B instability thermalize the directed ion motion by a process of quasi-linear velocity spreads in the velocity space to result in strong ion heating. Then, the relation of energy balance of ions may be given as follows;

$$\frac{d(nT_i)}{dt} = nR_H - \frac{i}{\tau_c} nT_i, \qquad (4)$$

with an ion confinement time τ_c. Equation (4) should be equal to zero in a steady state. Here the heating rate R_H may be given as

$$R_H = \frac{1}{\tau(k)} \frac{M}{2} (V_{eo}^2 + V_o^2) \qquad (5)$$

by using the effective collision time, $\tau(k)$, i.e. correlation

time mentioned above and the kinetic energy of ions is fed from the radial current and V_o is initial velocity of ions. R_H is also obtained by Ichimaru (1975) as

$$R_H = \frac{\partial U}{\partial t} = \frac{ne^2}{mv_o^2} \sum \frac{\langle |E_k|^2 \rangle}{k^2} \{ \nu(k) + (\frac{\pi}{2})^{1/2} \frac{|k \cdot V_d - \omega(k)|^2}{kv_o} \} \quad (6)$$

in our limiting case, where V_d is an average drift velocity. v_o is the velocity spread, and $\tau = 1/\nu(k)$ is the correlation time associated with the electric field fluctuations with wave vector k, and U is the density of thermal energy. The fluctuation wave energy $\langle |E_k|^2 \rangle / k^2$ is roughly proportional to the kinetic energy originated in the drift velocity, V_{eo}, because the linear growth rate is in proportion to V_{eo} as seen in Eq.(3). The first term in Eq.(6) shows the nonresonant scattering of ions from the fluctuating electric fields, while the second term stems from resonant coupling. Thus, we may obtain the expression for the ion temperature (Nishida et al, 1979)

$$T_i = \chi \cdot \tau_c \cdot R_H = \chi \cdot M(V_{eo}^2 + V_o^2) \tau_c / 2\tau, \quad (7)$$

where χ is assumed to be constant, but it would be a function of k. By the crude assumption of $V_H = E_{xo} R_o$, and R_o is the radius of the chamber in the heating section, T_i is seen to change roughly in proportion to V_H^2 as shown in Fig.5 by solid line which is actually calculated by using Eqs.(7) and (8) and the ion self-collision time, selfconsistently as will be discussed shortly later. The result shows reasonably good agreement, and thus the ion temperature is shown to increase in proportion to V_H^2.

An ion confinement time has been measured directly as already shown in Fig.7. If the ions with energy ε are confined in

the magnetic mirror field supplemented with axial and radial potential well for a time τ_c required for diffusing out by taking over the barrier height ϕ, τ_c may be given as follows in the present situation, similar to the result given by Pastukhov (1974),

$$\tau_c = \tau_i \ln R \left(\frac{\phi}{T_i}\right) \exp\left(\frac{\phi}{T_i}\right). \qquad (8)$$

When we take the ion self-collision time $\tau_i \simeq \tau$, which depends on the plasma density and the ion temperature as is well known (Spitzer, 1962), the ion temperature and the confinement time can be obtained self-consistently from Eqs.(7) and (8) in addition to the assumption of $\phi = aV_H$. An example is shwon by solid lines in Fig.7. Here, we also employed the parameter, a, which shows the effective height of the potential well being not decided self-consistently. The parameter, a, is selected to fit the calculated result of ion temperature with the experimental result at V_H = 1 kV. The result shown in Fig.7(b) shows reasonably good agreement with the experimental results, except for the ion confinement time around $V_H \simeq 200$ V, where the experimental result shows quite large confinement time. We cannot understand the mechanism of enhanced confinement at this small potential well. In a center region of the plasma column, however, we cannot employ the abovementioned model to interpret the confinement time, because in this region the plasma is fed from the discharge source region through the orifice O_2 and flown away by the centrifugal force toward the outer trapping region. Thus, the numerical results based on the abovementioned model does not fit with the experiments as seen in Fig.7(a). In the conven-

tional mirror machine, the ion confinement time τ_c is given as follows (Ioffe, 1965):

$$\tau_c = \frac{1}{\kappa} \frac{\sqrt{M}}{n} \frac{T_i^{3/2}}{\ln \Lambda} \ln R, \qquad (9)$$

where κ is a numerical factor of the order of unity depending on the shape of the magnetic field. $\ln \Lambda$ is the Coulomb logarithm (Spitzer, 1962). Equation (9) shows that τ_c increases with $T_i^{3/2}$ for constant other parameters determined by the machine. In our parameters at V_H = 1 kV, Eq.(9) gives the lifetime of about 0.1 msec, which is shorter than the observed values: thus the effect of the potential barrier for reducing the ion loss from the mirror throats is clear.

V Conclusion

Strong ion heating resulted from the EXB instability has been observed and the ion temperature increases in proportion to the square of the heating voltage V_H, i.e. proportional to the input DC power. The ion heating is resulted from the weak collision and/or finite correlation time of the strong EXB type instabilities. The increased ion confinement time is also observed along with the ion heating. These mechanism is understood by the ion trapping in a magnetic mirror field supplemented with the static electric field in the axial and radial directions. The maximum values of the applicable voltages across the plasma column for the increased heating and confinement time of ions are limited at present by the plasma breakdown. The discharge cleaning method was effective to decrease the impurities and as a

result to increase the maximum value of the breakdown voltages.

Acknowledgements

The present work was performed under the auspieces of Collaborating Research Program at Institute of Plasma Physics, Nagoya University. One of the authors (YN) is indebted to the Ministry of Education, Science and Culture, Japan, that supported a part of the present work by the Grant-in-Aid for the Scientific Research.

References

* permanent address: Department of Electrical Engineering, Utsunomiya University, Utsunomiya, Tochigi 321, Japan.

**permanent address: Department of Electronic Engineering, Ibaragi University, Hitachi, Ibaragi 316, Japan.

Alexeff I. et al (1970) Phys. Rev. Lett. 25 848.

Alikhanov S.G., I.K. Konkashbaev, and P.Z. Chebatov (1970) Nucl. Fusion 10 13.

Alikhanov S.G. and I.K. Konkashbaev (1974) Nucl. Fusion 14 34.

Dimov G.I., V.V. Zakaidakov, and M.E. Kishinevskii (1976) Sov. J. Plasma Phys. 2 326.

Fowler T.K. (1981) Fusion ed. by E. Teller, Academic Press, vol.1 Part A, p.291.

Ichimaru S. (1975) J. Phys. Soc. Japan 39 1373.

Ioffe M.S. (1965) Plasma Physics (International Atomic Energy Agency, Vienna) p.421.

Nishida Y., Y. Hatta, and M. Sato (1968) J. Phys. Soc. Japan 24 923.

Nishida Y. and Y. Hatta (1970) J. Phys. Soc. Japan 29 1341.

Nishida Y., S. Kawamata, and K. Ishii (1975) Proceedings of 7th European Conference on Controlled Fusion and Plasma Physics, Lausanne, Vol.1, p.34.

Nishida Y., S. Kawamata, and K. Ishii (1977) J. Phys. Soc. Japan 43 1364.

Nishida Y., H. Mase, and K. Ishii (1979) Proceedings of 9th European Conference on Controlled Fusion and Plasma Physics,

Oxford.

Pastukhov V.P. (1974) Nucl. Fusion 14 3.

Roth J. (1973) Phys. Fluids 16 231.

Saito S., N. Sato, and Y. Hatta (1966) J. Phys. Soc. Japan 21 2695.

Spitzer L. (1962) Physics of Fully Ionized Gases, Wiley. Interscience, New York.

Sugai H. et al (1977) J. Phys. Soc. Japan 43 1400.

Takayama K., M. Otsuka, Y. Tanaka, K. Ishii, and Y. Kubota (1967) Proceedings of the 8th International Conference of Phenomena in Ionized Gases, Vienna, Springer, Berlin, p.551.

Figure captions

Fig.1. Schematic description of the experimental apparatus. P_L is either Langmuir probe or floating double probe system. P_2 is a Langmuir probe.

Fig.2. Ion loss factor, δ, vs. the applied heating voltage V_H in the discharge current ——: I_d = 10 A. — — —: I_d = 20 A. – – – – –: I_d = 30 A and —— — —: I_d = 50 A. B_{max} = 4.6 kG and P $\simeq$ (0.7-1.0) x 10^{-3} Torr.

Fig.3. Observed raw data of the spectrum around He..(4686 A) line.

Fig.4. Line intensity vs. the difference of spectrum line, $\Delta\lambda$, measured from HeII line.

Fig.5. Ion temperature T_i as a function of heating voltage V_H. Open circles correspond to the high energy tail and closed circles to the bulk component, respectively. Solid line is calculated with Eqs.(7) and (8).

Fig.6. Plasma breakdown voltage V_B vs. the neutral gas pressure. R_o is the radius of the chamber. Closed circles correspond to R_o = 6 cm, open circles to R_o = 7.5 cm and triangles to R_o = 5 cm, respectively.

Fig.7. Observed particle confinement time as a function of the heating voltage obtained in a dilute plasma of density 10^{11} cm^{-3}. (a) the results observed at r = 1 cm, inside of the plasma core region, and (b) at r = 7 cm, outer trapping section. Solid line is calculated from Eqs.(7) and (8).

Fig.8. An example of the observed instability spectrum in the trapping section.

Fig.9. Analyzed data of the instability-spectrum observed in several conditions. Solid lines correspond to m = 1 and m = 2 modes.

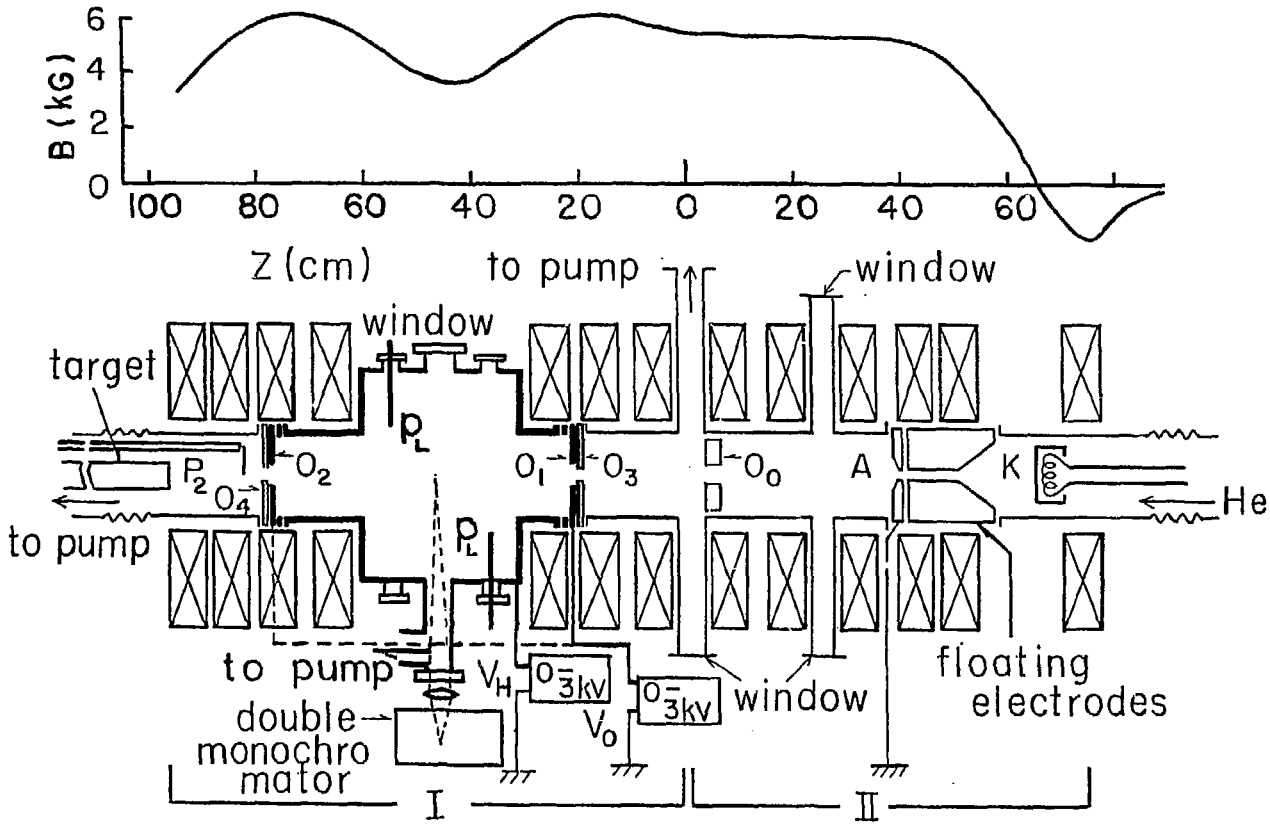
B (kG)
6
4
2
0
100
80
60
40
20
0
20
40
60
Z (cm)
to pump
window
window
target
P_L
P_2
O_4
O_2
O_1
O_3
O_0
A
K
He
to pump
P_L
to pump
V_H
O_{-3kV}
V_0
O_{-3kV}
window
floating
electrodes
double
monochro
mator
I
II

FIG. 1

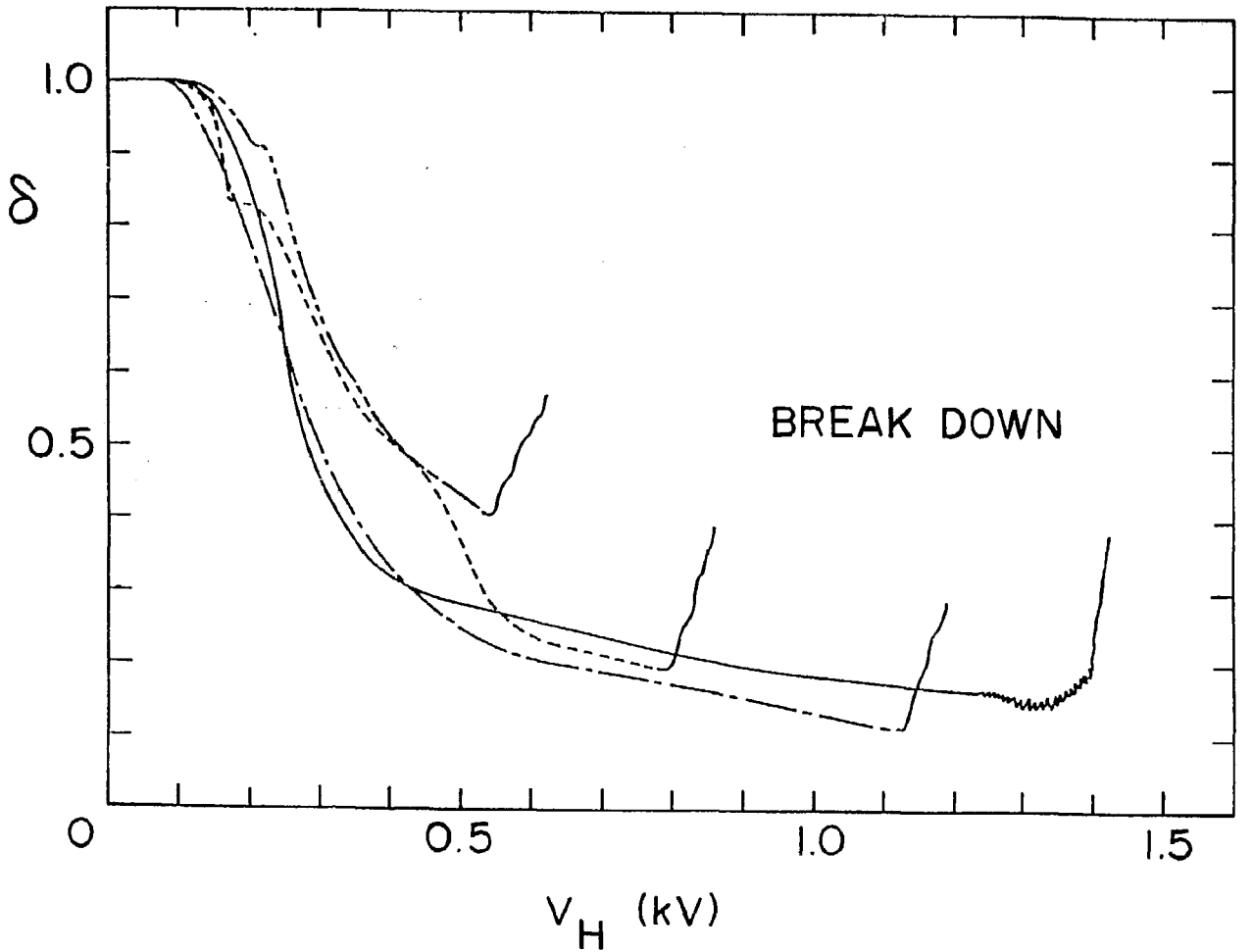

FIG. 2

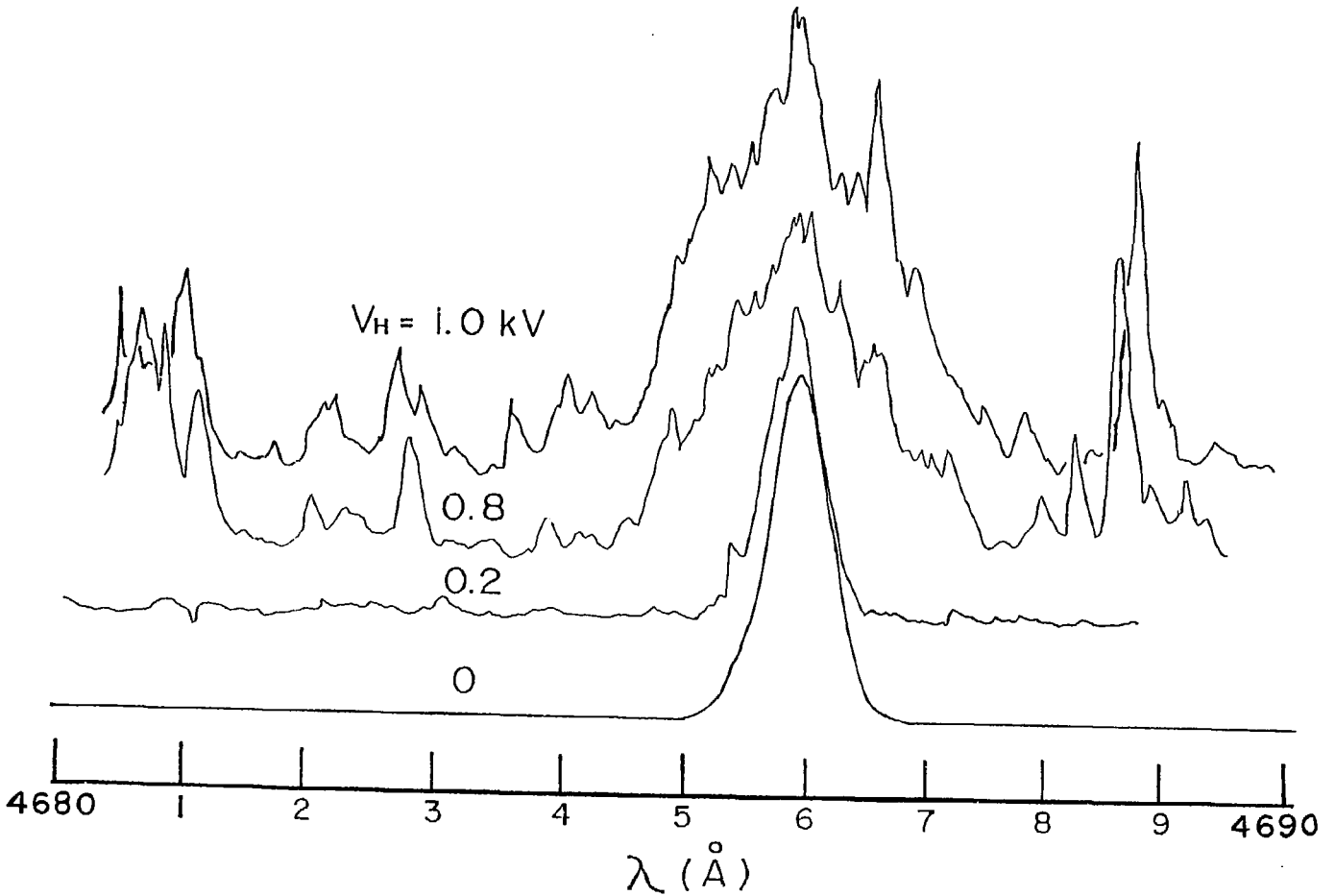

FIG. 3

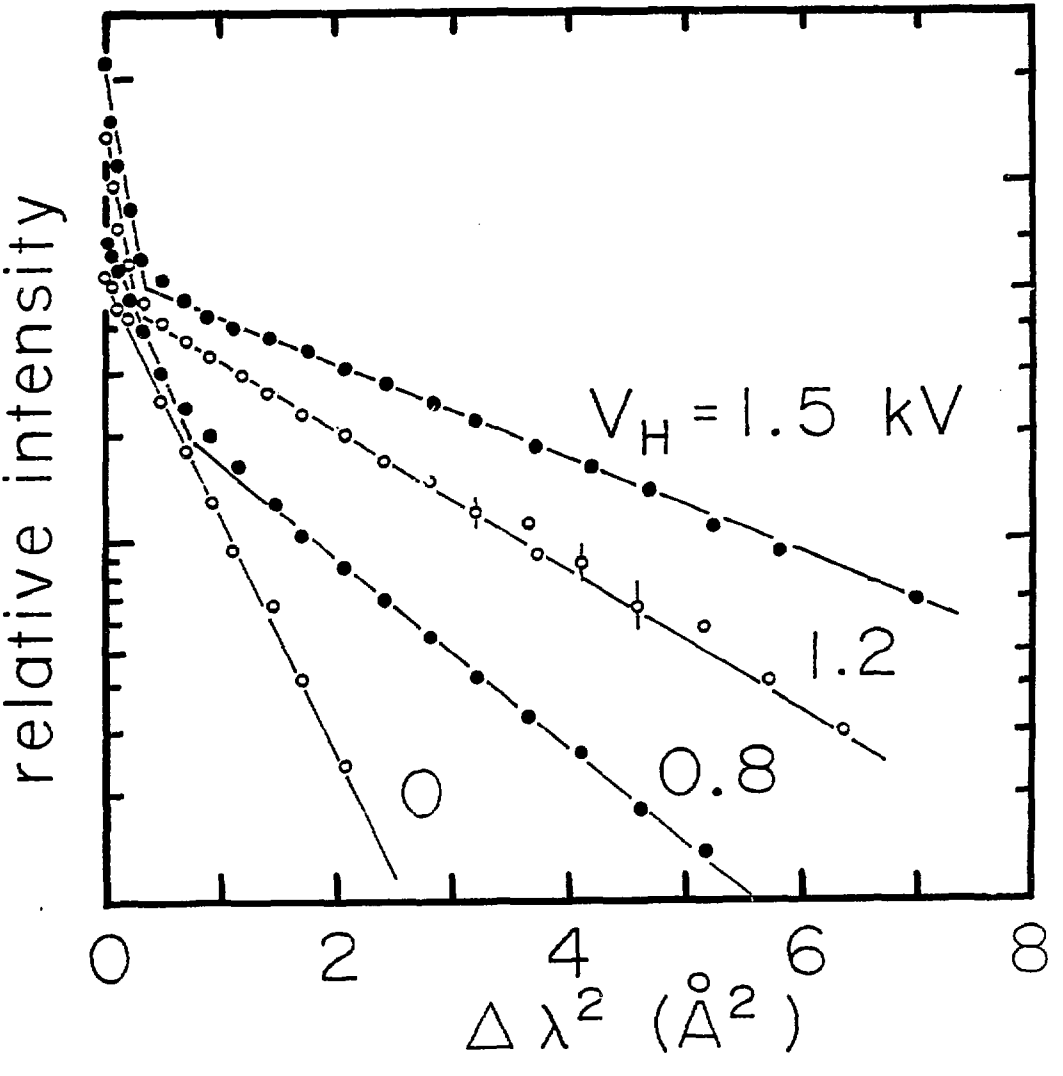

FIG. 4

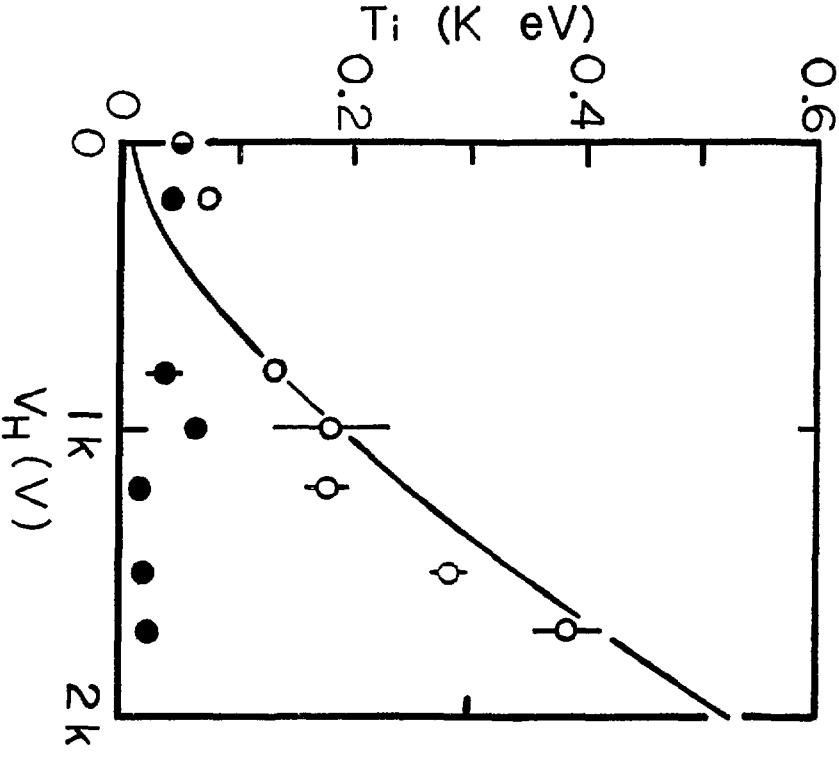

FIG. 5

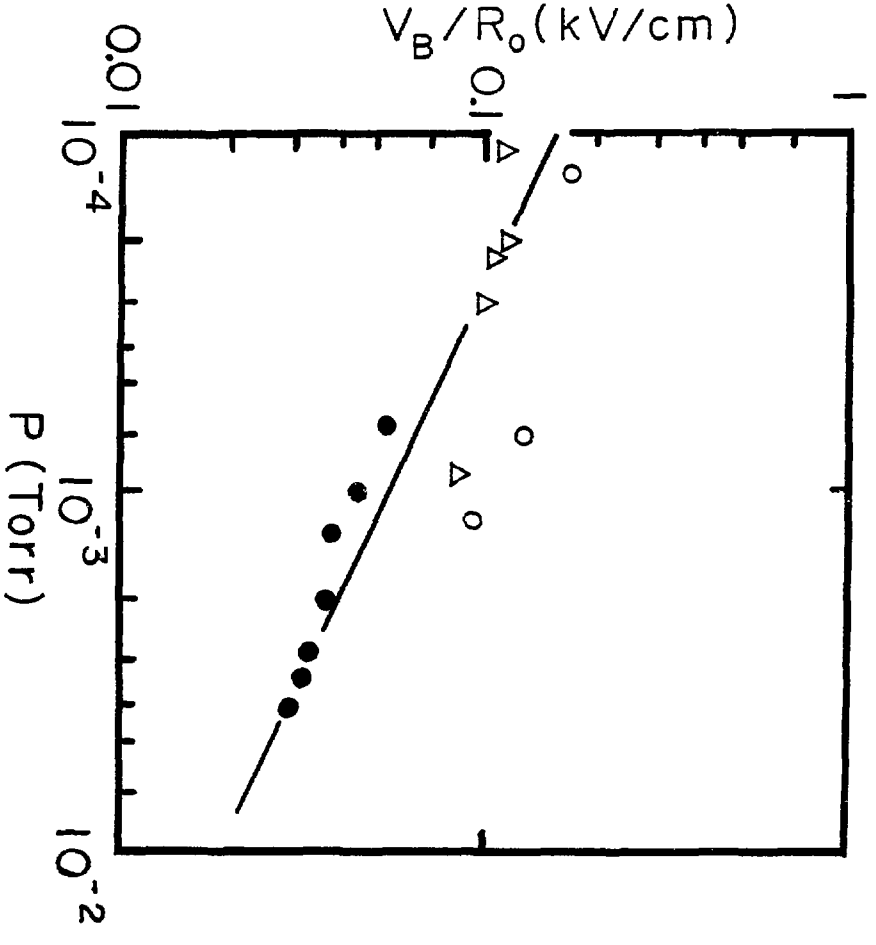

FIG. 6

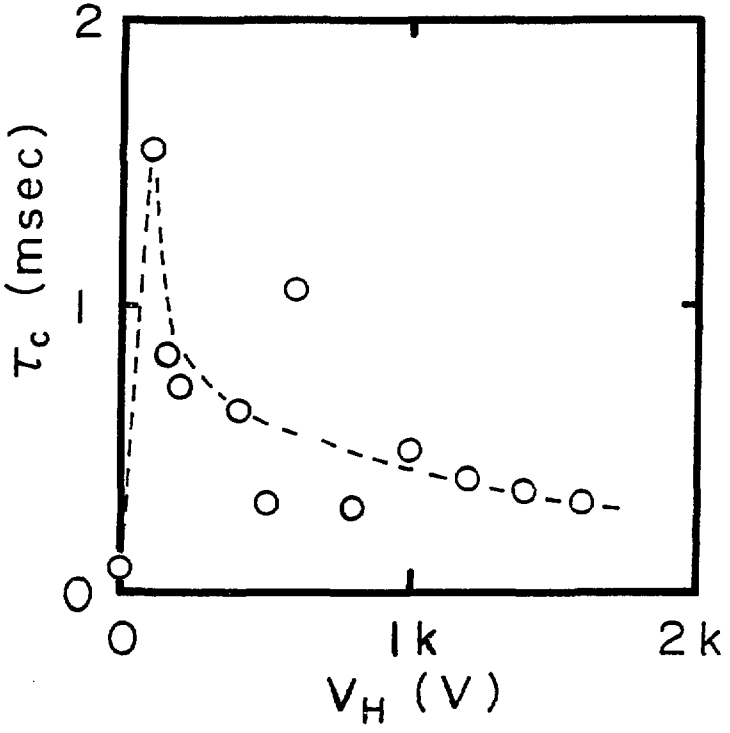

FIG. 7 (A)

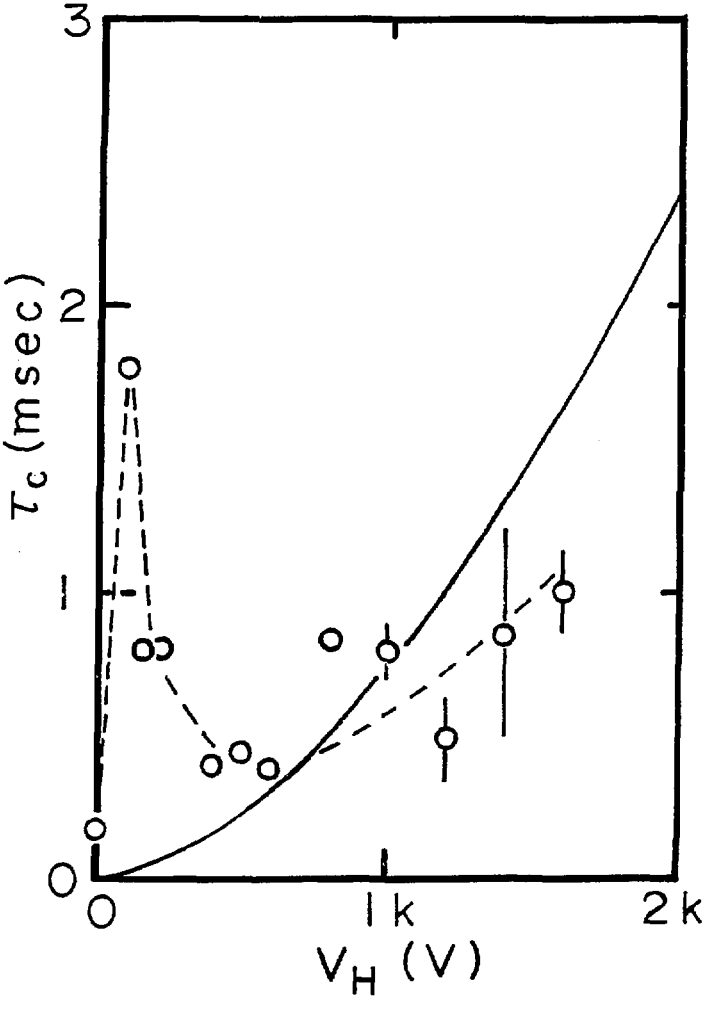

FIG. 7 (B)

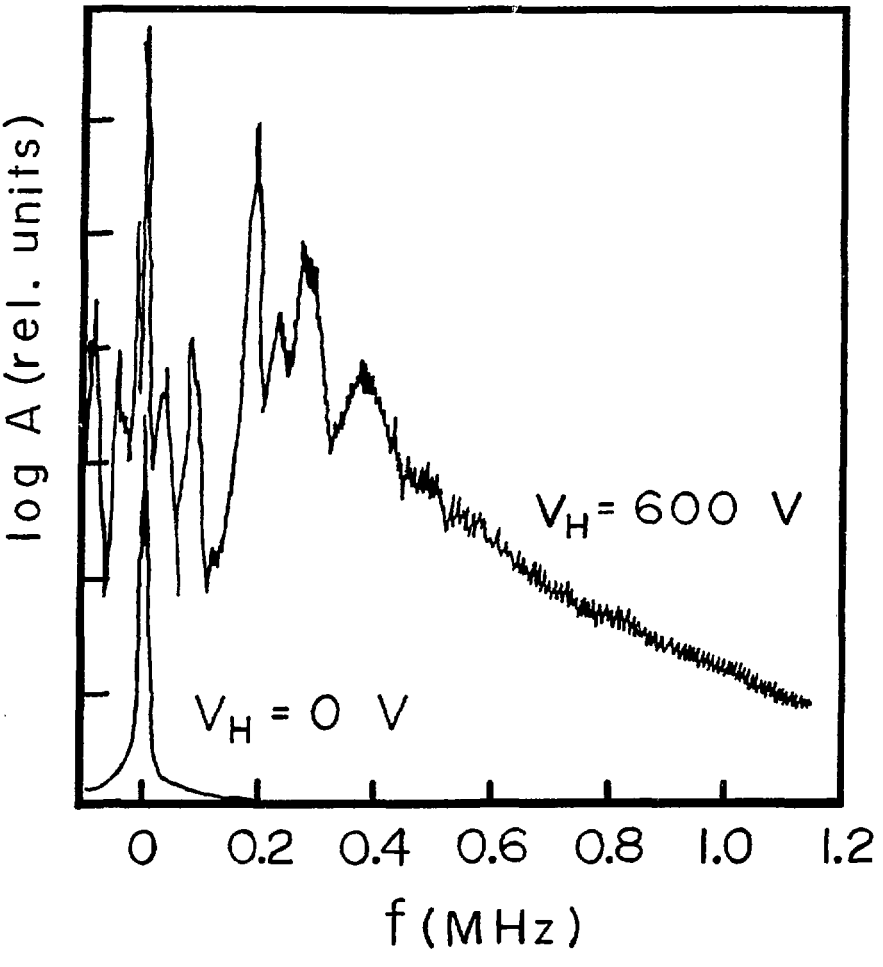

FIG. 8

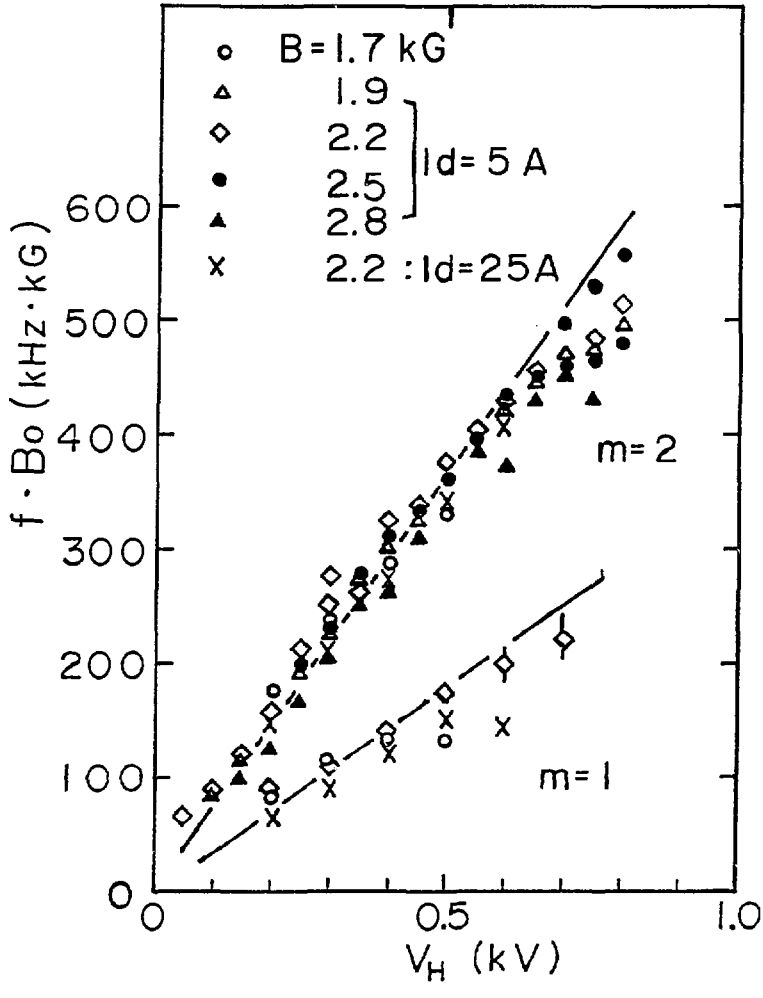
B=1.7 kG
1.9
2.2
2.5
2.8
Id=5 A
2.2 : Id=25A
m=2
m=1
f·Bo (kHz·kG)
600
500
400
300
200
100
0
0
0.5
1.0
VH (kV)

FIG. 9